ChemComm

COMMUNICATION

View Article Online
View Journal | View Issue

Cite this: *Chem. Commun.*, 2014, 50, 14325

Received 9th March 2014,
Accepted 24th September 2014

DOI: 10.1039/c4cc01773k

www.rsc.org/chemcomm

High-yield synthesis and crystal structure of a green Au_{30} cluster co-capped by thiolate and sulfide†

Huayan Yang,‡[a] Yu Wang,‡[a] Alison J. Edwards,[b] Juanzhu Yan[a] and Nanfeng Zheng*[a]

A green gold-cluster, $Au_{30}S(StBu)_{18}$, was successfully prepared in high yield and crystallographically characterized. Each cluster consists of an Au_{22} core capped by a mixed layer of staple Au-thiolate units, bridging thiolates and a μ_3-S^{2-}.

Since the crystallographic structure determination of $Au_{102}(p\text{-MBA})_{44}$ in 2007,[1] thiolate-stabilized metal nanoclusters have attracted increasing research attention owing to their well-defined molecular structures.[2–7] A series of atomically precise thiolated/selenolated Au nanoclusters have been synthesized and crystallographically characterized.[8–13] In reported thiolated Au nanoclusters, staple $Au_x(SR)_{x+1}$ units are commonly observed in their surface protected layers. Numerous subsequent studies have demonstrated the influence of both the metal species in the core and capping ligands on the surface features of thiolated metal nanoclusters. No staple units were revealed on the surfaces of thiolated metal nanoclusters where metals other than Au were introduced. Ag_{44} and $Au_{12}Ag_{32}$ clusters reported to date do not include staple units.[14–16] Non-staple units were proposed on the surface of $Au_{41}(S\text{-Eind})_{12}$ where a bulky thiol is used.[17] A μ_3-like bonding of that ligand to Au was suggested. The potential for a diverse array of structure motifs beyond simple $Au_x(SR)_{x+1}$ staple units is envisaged to enrich the structures of thiolated metal nanoparticles and expand the range of surface properties beyond those of known thiolated-Au nanoclusters.[17,18]

Here we report the high-yield synthesis of $Au_{30}S(StBu)_{18}$ and its crystal structure. A trace amount of Na_2S is used as the S^{2-} source to explore incorporation of S^{2-} on the surface of thiolated nanoclusters. The crystal structure analysis reveals that each cluster comprises an Au_{22} core capped by a mixed layer of staple Au-thiolate units, bridging thiolates and a μ_3-S^{2-}. As part of the surface protecting layer, S^{2-} serves as a μ_3-ligand coordinating to three Au atoms. The structure of $Au_{30}S(StBu)_{18}$ gives direct evidence that μ_3-S^{2-} readily acts as a surface protecting ligand to introduce a new surface structure giving potential for preparing more structurally diverse thiolated Au nanoclusters.

To incorporate S^{2-} onto the surface of thiolated Au nanoclusters, Na_2S was introduced deliberately in the synthesis of Au nanoclusters. In a typical synthesis of $Au_{30}S(StBu)_{18}$ nanoclusters (ESI†), $HAuCl_4$ and *tert*-butylthiol (t-C_4H_9SH) (1 : 3 molar ratio) were combined in tetrahydrofuran (THF). After stirring for 15 min at 55 °C, aqueous solutions of $NaBH_4$ and Na_2S were added simultaneously into the mixture of $HAuCl_4$ and t-C_4H_9SH. The ratio of $HAuCl_4$: $NaBH_4$: Na_2S was 50 : 500 : 1. The reaction mixture turned dark-brown immediately and was kept under stirring at 55 °C for another hour. After the aqueous layer was removed, toluene and excess t-C_4H_9SH were added to the reaction mixture whose temperature was then raised to 60 °C. The colour of the solution gradually changed from dark-brown to dark-green in the following 6 h stirring at 60 °C. Brown sheet-like single crystals of $Au_{30}S(StBu)_{18}$ were recrystallized by diffusing hexane into the cluster solution in CH_2Cl_2 at 4 °C over 15 days. The crystals were readily redissolved in toluene to give a green solution.

The molecular structure of $Au_{30}S(StBu)_{18}$ was determined by X-ray single crystal analysis.§ $Au_{30}S(StBu)_{18}$ clusters are crystallized in the triclinic space group $P\bar{1}$ (Fig. S1, ESI†). As illustrated in Fig. 1 and Fig. S2 (ESI†), $Au_{30}S(StBu)_{18}$ is formulated as a neutral cluster with a rod-like Au_{22} core capped by a mixed layer of thiolate ligands, gold–thiolate complex units and S^{2-}. The mixed surface capping layer consists of two $Au_3(SR)_4$ staple units, two $Au(SR)_2$ units, six bridging thiolate SR ligands and one S^{2-}. Although the Au-thiolate staple units[1,8–12] and bridging thiolates[10] have been previously revealed as important surface capping motifs in the reported structures of thiolated-Au nanoclusters, the presence of surface μ_3-S^{2-} motifs has not been previously observed in thiolated Au nanoclusters.

[a] *State Key Laboratory for Physical Chemistry of Solid Surfaces and Department of Chemistry, Xiamen University, Xiamen 361005, China. E-mail: nfzheng@xmu.edu.cn; Web: http://chem.xmu.edu.cn/groupweb/nfzheng/index.asp; Fax: +86 592 2183047; Tel: +86 592 2186821*

[b] *Bragg Institute, Australian Nuclear Science and Technology Organization, New Illawarra Road, Lucas Heights, New South Wales 2234, Australia*

† Electronic supplementary information (ESI) available: Experimental details and crystallographic data, and the MALDI mass spectra of pure $Au_{30}S(StBu)_{18}$ with the laser irradiation of increased power. CCDC 986161. For ESI and crystallographic data in CIF or other electronic format see DOI: 10.1039/c4cc01773k

‡ H.Y. and Y.W. contributed equally to this work.

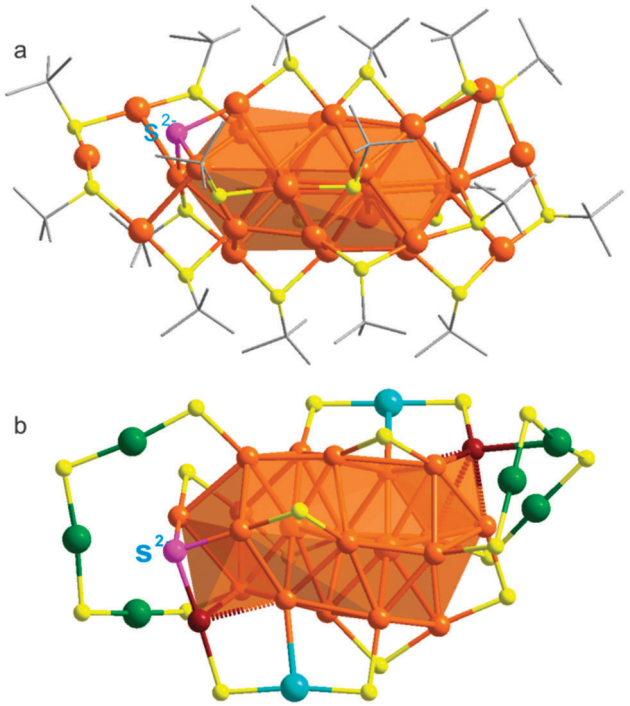

Fig. 1 The molecular structure of $Au_{30}S(StBu)_{18}$ from X-ray diffraction analysis. All hydrogen (a, b) and carbon (b) atoms are omitted for clarity. Colour legend: orange/green/cyan/red spheres, Au; pink sphere, S^{2-}; yellow sphere, S on thiolate; grey stick, C.

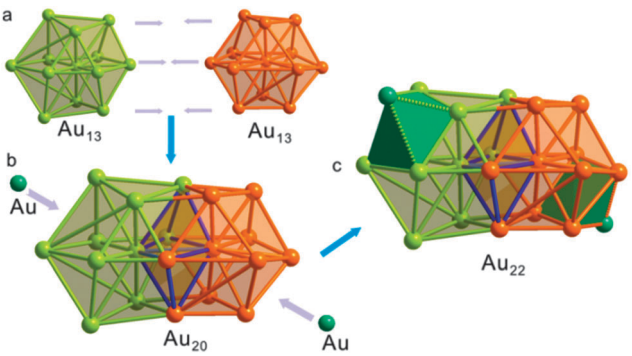

Fig. 2 (a, b) The structure of Au_{20} in the Au_{22} core. (c) The overall structure of the Au_{22} core. Colour legend: orange/yellow-green spheres, Au atoms of Au_{20} bicuboctahedron; green sphere, the two capping Au atoms of Au_{22}.

As depicted in Fig. 2, the Au_{22} core of $Au_{30}S(StBu)_{18}$ can be better described structurally as a rod-like Au_{20} unit face-capped by two Au atoms. Au_{20} is a bicuboctahedral unit consisting of two distorted interpenetrating Au_{13} cuboctahedrons, similar to the Au_{20} core of $Au_{28}(TBBT)_{20}$.[10] In the core of $Au_{30}S(StBu)_{18}$, however, the Au_{20} unit is further face-capped by two Au atoms at either end, resulting in the formation of a rod-like Au_{22} core. The average Au–Au bond length of the Au_{20} bicuboctahedron is 2.89 Å which is comparable to the bond length in bulk gold (2.88 Å) and shorter than the bond length of the Au_{20} kernel of Au_{28} (2.92 Å).

The presence of two additional face-capping Au atoms (Au_{cap}) in the core of $Au_{30}S(StBu)_{18}$ significantly modifies the surface binding structure when compared with that of $Au_{28}(TBBT)_{20}$.[10] While the Au_{20} core in $Au_{28}(TBBT)_{20}$ is protected by four $Au_2(SR)_3$ staple units and eight bridging SR ligands, no comparable $Au_2(SR)_3$ staple units are revealed on the surface of $Au_{30}S(StBu)_{18}$ for which a diversity of surface motifs are identified. As shown in Fig. 1b and Fig. S3 (ESI†), each of the two $Au_3(SR)_4$ staple units is capping an end of the Au_{22} core with the terminal thiolates binding to Au atoms on the bicuboctahedral unit. The two $Au(SR)_2$ units bind at the sides of the rod-like Au_{22} core with one thiolate coordinating to an Au atom on the bicuboctahedral unit and the other to a capping Au atom. Similar to the situation in $[Au_{23}(SC_6H_{11})_{16}]^-$,[12] each of the two face-capping Au atoms in the core forms a linker between the $Au_3(SR)_4$ and $Au(SR)_2$ units. The Au_{22} core is further bound by four bridging SR at its sides, two bridging SR ligands on both ends, and one μ_3-S^{2-} on one end. The average Au–S bond length/Au–S–Au bond angle are 2.311 Å/96.281° and 2.330 Å/97.337° in the $Au_3(SR)_4$ and $Au(SR)_2$ units, respectively. Compared with those in staple units, the average Au–S–Au bond angle (92.22°) at the six bridging SR ligands is smaller and their average Au–S bond length (2.338 Å) is slightly longer.

Only one μ_3-S^{2-} is present on the surface of $Au_{30}S(StBu)_{18}$, rendering the cluster asymmetric due to its location at one end of the Au_{22} core. The μ_3-S^{2-} binds to two adjacent Au atoms on the bicuboctahedral Au_{20} unit and to one Au_{cap} atom as described above. Such a coordination mode differentiates the binding structures of the two face-capping Au atoms in the Au_{22} core. While the Au_{cap} at the end without μ_3-S^{2-} binding caps an Au_4 square, the other Au_{cap} only caps three Au atoms of the bicuboctahedral unit. Although observed in small Au clusters,[19] the presence of μ_3-S^{2-} surface motifs has not been well reported in large thiolated Au nanoclusters. The unique μ_3-coordinated sulfide on an Au cluster presents an opportunity to create custom-modified thiolated Au nanoclusters with the potential for targeted functionality and applications.

As illustrated in Fig. 3a, the UV-Vis spectrum of $Au_{30}S(StBu)_{18}$ in toluene displays one major absorption peak at 620 nm and two shoulder peaks around 375 nm and 475 nm (Fig. 3b). Such an optical absorption of $Au_{30}S(StBu)_{18}$ is very similar to that of the all-thiolate-protected $Au_{30}(S\text{-}tBu)_{18}$ cluster.[20] Very recently, Dass and coworkers also obtained single crystals of $Au_{30}S(StBu)_{18}$ during the crystallization of chromatographically purified $Au_{30}(StBu)_{18}$.[21] With the use of a trace amount of Na_2S, we demonstrate a high-yield, high-purity synthesis of $Au_{30}S(StBu)_{18}$ in a one-pot method

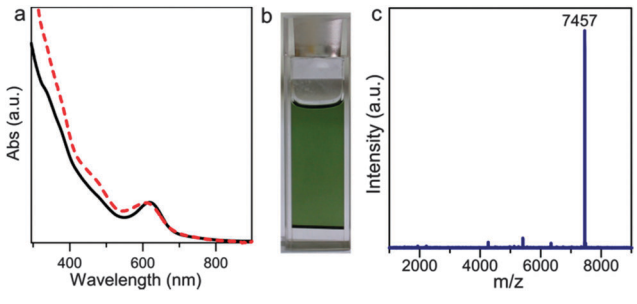

Fig. 3 (a) The UV/vis absorption spectra of $Au_{30}S(StBu)_{18}$; the black line is pure $Au_{30}S(StBu)_{18}$ dissolved in CH_2Cl_2 and the red dashed line is the crude product in a mixed solvent of toluene and THF. (b) A photo of $Au_{30}S(StBu)_{18}$ in toluene. (c) The MALDI mass spectrum of pure $Au_{30}S(StBu)_{18}$ clusters from dissolved crystals.

without purification. The crude reaction product of this synthesis displayed an identical UV-Vis absorption to that of single crystals of $Au_{30}S(StBu)_{18}$ dissolved in CH_2Cl_2 (Fig. 3a). To confirm the high purity of $Au_{30}S(StBu)_{18}$ in the reaction mixture, the mass spectra of both the crude product and the pure crystals were further analysed. A clean and strong peak with *m*/*z* of 7457 is clearly observed in both mass spectra (Fig. 3c and Fig. S4, ESI†). The peak is assigned to $[Au_{30}S(StBu)_{17}]^+$ which corresponds to the loss of one $StBu^-$ group from the $Au_{30}S(StBu)_{18}$ cluster. These results demonstrate the high purity of $Au_{30}S(StBu)_{18}$ in the crude product. When the laser intensity used in the MALDI-MS measurements was increased, further loss of organic ligands from the cluster was observed (Fig. S5, ESI†). The high-yield production of $Au_{30}S(StBu)_{18}$ on introducing Na_2S could be rationalized by the presence of μ_3-S^{2-} which helps to relieve the steric pressure caused by the adjacent five S*t*Bu groups. It should be noted that $Au_{30}S(StBu)_{18}$ is not luminescent while strongly absorbing in the UV-Vis region.

In conclusion, a new gold-nanocluster, $Au_{30}S(StBu)_{18}$, was successfully synthesized and structurally determined by single crystal analysis. The introduction of a trace amount of Na_2S was found to be critical for achieving the high-yield synthesis of $Au_{30}S(StBu)_{18}$. While the core of $Au_{30}S(StBu)_{18}$ is an Au_{22} unit that can be described as a bicuboctahedral Au_{20} unit capped by two Au atoms, the surface layer of the cluster consists of two $Au_3(SR)_4$ staple units, two $Au(SR)_2$ units, six bridging SR ligands and one μ_3-S^{2-}. The presence of μ_3-S^{2-} on a thiolated Au nanocluster provides opportunities to create and manipulate surface structures of thiolated Au nanoparticles.

We thank the Ministry of Science and Technology of China (2011CB932403) and the National Natural Science Foundation of China (21131005, 21420102001, 21390390, 21227001) for financial support.

Notes and references

§ The diffraction patterns measured for the compound are dominated by the scattering from the $Au_{30}S_{19}$ core with almost 3000 electrons whereas the less ordered tertiary butyl shell contains fewer than 600 electrons distributed in a considerably large volume. The structure analysis is complicated by the occurrence of twinning which appears to be an inherent property of crystals of this material. Review of the diffraction images confirmed this diagnosis and calculated precession layers demonstrated that additional smaller twin components may also be present. Residual electron density in the core region is ascribed to minor twin components which were not modeled. A large void in the structure, ~22% of the cell volume, has a calculated electron content of ~400 and is consistent with occupation by disordered solvent. A detailed description of the structure analysis is provided in the CIF.

1 P. D. Jadzinsky, G. Calero, C. J. Ackerson, D. A. Bushnell and R. D. Kornberg, *Science*, 2007, **318**, 430.
2 H. Qian, M. Zhu, Z. Wu and R. Jin, *Acc. Chem. Res.*, 2012, **45**, 1470–1479.
3 P. Maity, S. Xie, M. Yamauchi and T. Tsukuda, *Nanoscale*, 2012, **4**, 4027–4037.
4 D. Jiang, *Nanoscale*, 2013, **5**, 7149–7160.
5 H. Häkkinen, *Nat. Chem.*, 2012, **4**, 443–455.
6 Y. Yu, Z. Luo, D. M. Chevrier, D. T. Leong, P. Zhang, D.-e. Jiang and J. Xie, *J. Am. Chem. Soc.*, 2014, **136**, 1246–1249.
7 R. Jin and K. Nobusada, *Nano Res.*, 2014, **7**, 285–300.
8 H. F. Qian, W. T. Eckenhoff, Y. Zhu, T. Pintauer and R. C. Jin, *J. Am. Chem. Soc.*, 2010, **132**, 8280–8281.
9 M. W. Heaven, A. Dass, P. S. White, K. M. Holt and R. W. Murray, *J. Am. Chem. Soc.*, 2008, **130**, 3754–3755.
10 C. J. Zeng, T. Li, A. Das, N. L. Rosi and R. C. Jin, *J. Am. Chem. Soc.*, 2013, **135**, 10011–10013.
11 M. Z. Zhu, C. M. Aikens, F. J. Hollander, G. C. Schatz and R. Jin, *J. Am. Chem. Soc.*, 2008, **130**, 5883–5885.
12 A. Das, T. Li, K. Nobusada, C. Zeng, N. L. Rosi and R. Jin, *J. Am. Chem. Soc.*, 2013, **135**, 18264–18267.
13 Y. Song, S. Wang, J. Zhang, X. Kang, S. Chen, P. Li, H. Sheng and M. Zhu, *J. Am. Chem. Soc.*, 2014, **136**, 2963–2965.
14 H. Y. Yang, Y. Wang, H. Q. Huang, L. Gell, L. Lehtovaara, S. Malola, H. Häkkinen and N. F. Zheng, *Nat. Commun.*, 2013, **4**, 2422.
15 X. Zhang, H. Y. Yang, X. J. Zhao, Y. Wang and N. F. Zheng, *Chin. Chem. Lett.*, 2014, **25**, 839–843.
16 A. Desireddy, B. E. Conn, J. Guo, B. Yoon, R. N. Barnett, B. M. Monahan, K. Kirschbaum, W. P. Griffith, R. L. Whetten, U. Landman and T. P. Bigioni, *Nature*, 2013, **501**, 399–402.
17 J. Nishigaki, R. Tsunoyama, H. Tsunoyama, N. Ichikuni, S. Yamazoe, Y. Negishi, M. Ito, T. Matsuo, K. Tamao and T. Tsukuda, *J. Am. Chem. Soc.*, 2012, **134**, 14295–14297.
18 P. J. Krommenhoek, J. Wang, N. Hentz, A. C. Johnston-Peck, K. A. Kozek, G. Kalyuzhny and J. B. Tracy, *ACS Nano*, 2012, **6**, 4903–4911.
19 Q.-M. Wang, Y.-A. Lee, O. Crespo, J. Deaton, C. Tang, H. J. Gysling, M. Concepción Gimeno, C. Larraz, M. D. Villacampa, A. Laguna and R. Eisenberg, *J. Am. Chem. Soc.*, 2004, **126**, 9488–9489.
20 D. Crasto and A. Dass, *J. Phys. Chem. C*, 2013, **117**, 22094–22097.
21 D. Crasto, S. Malola, G. Brosofsky, A. Dass and H. Häkkinen, *J. Am. Chem. Soc.*, 2014, **136**, 5000–5005.